Influence of 5-Fluorouracil–Loaded Microsphere Formulation on Efficient Rat Glioma Radiosensitization

Valérie-Gaëlle Roullin,[1] Martine Mege,[2] Laurent Lemaire,[1] Jean-Pierre Cueyssac,[2] Marie-Claire Venier-Julienne,[1] Philippe Menei,[1,3] Erik Gamelin,[2] and Jean-Pierre Benoit[1,4]

Received February 17, 2004; accepted May 17, 2004

Purpose. To determine (i) the efficiency of radiosensitizing 5-FU–loaded microspheres and (ii) the impact of microparticle formulation on response to treatment.

Methods. C6 tumor-bearing rats were stereotactically implanted with microspheres and/or allocated to: control groups (untreated) or treatment (only radiotherapy; fast-release 5-FU microspheres + radiotherapy; slow-release 5-FU microspheres + radiotherapy). The next day, fractionated radiotherapy, limited to the hemibrain, was initiated in all treated animals. The irradiation cycle included 36 Gy, given in 9 sessions for 3 consecutive weeks. Tumor development was assessed by T_2-weighted MRI.

Results. 5-FU microspheres associated with radiotherapy caused a 47% complete remission rate (9/19) as opposed to the 8% rate (1/12) when radiotherapy alone or 0% in control animals. Drug delivery for 3 weeks produced better survival results (57%) compared to one-week sustained release (41%). MR images showed exponentially increasing tumor volumes during the first half of the radiotherapy cycle, followed by a decrease, and the disappearance of the tumor if survival exceeded 120 days.

Conclusions. 5-FU controlled delivery is a promising strategy for radiosensitizing gliomas. Drug delivery system formulation is unambiguously implicated in both the response to treatment and the limitation of toxic side effects.

KEY WORDS: 5-fluorouracil; glioma; microspheres; MRI; radiosensitization.

INTRODUCTION

Glioblastoma, a highly malignant brain tumor, usually has a poor prognosis despite surgical treatment, radiation therapy, and/or systemic chemotherapy (1–2). Indeed, survival medians after surgery and radiotherapy are only 9–12 months (3). Among many substantial efforts produced to fight against this challenge, an increase in the efficiency of radiotherapy is certainly a promising way to obtain better results. The radiosensitization of tumor cells is one part of the strategy. Various molecules have been described as radiosensitizers (4–5), the most often cited in clinics being carmustin (6), platinum compounds (7) and halogenated pyrimidines (8), including 5-fluorouracil (5-FU) (9–10). To be really effective, a radiosensitizer has to be tumor-toxic and present in a sufficient concentration locally for at least 24 h post-irradiation (8,11). With this in mind, microspheres constitute an efficient means to reach these goals. Loaded with the radiosensitizer 5-FU, they allow its local sustained release over a variable period of time, while avoiding systemic toxicity. Such microspheres have been successfully designed in our laboratory (12), presenting various *in vitro* kinetics according to their formulation. In previous works, their superiority *per se* over an intracerebral bolus of 5-FU, as well as dose and formulation optimization, has been determined in an established C6-glioma model (13–14). Two formulations were particularly interesting in terms of survival data (15) and we wished, in the present study, to examine (i) the therapeutic potency of these microspheres when associated with a radiotherapy scheme used in clinics and (ii) the impact of microsphere formulations upon a response to treatment, as assessed by tumor volume follow-up using magnetic resonance imaging (MRI).

MATERIALS AND METHODS

Animals and C6-Cell Inoculation

Forty-three Sprague-Dawley female rats, with 160–200 g body weight (Elevages Dépré, St Doulchard, France), were used in this study. They were housed in standard animal facilities and given free access to water and food. Animal care protocols were performed in strict accordance with the local ethics guidelines and in compliance with the Guide for the Care and Use of Laboratory Animals (U.S. National Institutes of Health, revised 1996).

The C6-glioma tumor line used in this study and the cell inoculation procedure have been described elsewhere (16). Briefly, anaesthetized animals were placed in a stereotactic head frame (Stoelting, Wood Dale, USA) and a burr hole was drilled (anterior 0 mm, lateral 3 mm, depth 7 mm, according to the bregma). The cell suspension, in a state of exponential growth, was inoculated over a 10-min period (4×10^4 C6 cells in 10 μl DMEM). The scalp was closed with surgical thread. Tumors were allowed 12 days to develop before they presented a mean volume of 20 mm^3 (16).

Microsphere Preparation and Implantation

Microspheres were prepared by the solvent evaporation/extraction method, as previously reported (12). Briefly, 5-FU crystals were suspended in a poly(lactide-*co*-glycolide) (PLGA 50/50)/methylene chloride/acetone solution and poured into a poly(vinylalcohol) (PVA) aqueous solution under mechanical stirring. The emulsion was added to water, still under mechanical stirring, allowing solvent extraction to take place. Fast-release microspheres (MS-F, containing 23.7% 5-FU) exhibited 58% drug release in 24 h and a 100% drug release within 7 days; slow-release microspheres (MS-S, containing 21.3% 5-FU) were characterized by a 28% drug release in 24 h and a 100% drug release within 20 days (15). The two different formulations were obtained by modifying some emulsion/extraction parameters: the drug/polymer ratio (1 for MS-F, 0.8 for MS-S), the polymer/methylene chloride

[1] INSERM ERIT-M 0104, 49100 Angers, France.
[2] Centre Paul Papin, 49100 Angers, France.
[3] Service de Neurochirurgie, Centre Hospitalier Universitaire, 49100 Angers, France.
[4] To whom correspondence should be addressed. (e-mail: jean-pierre.benoit@univ-angers.fr)

ABBREVIATIONS: 5-FU, 5-fluorouracil ; MRI, magnetic resonance imaging ; MS, microspheres; RDT, radiotherapy.

0724-8741/04/0900-1558/0

ratio (0.08 for MS-F, 0.11 for MS-S), the emulsion/extraction volume ratio (0.17 for MS-F, 0.34 for MS-S) and the emulsion speed (750 rpm for MS-F vs 13,500rpm for MS-S). For implantation purposes, microspheres were suspended in a sodium-carboxymethylcellulose (CMC) sterile solution (1.2% CMC, 0.9% polysorbate 80, 3.8% mannitol, all w/w). On Day 12 post-inoculation, microsphere suspensions (20μl) were injected at the same coordinates as those used for tumor cells, at the rate of 1μl per minute. Microsphere concentrations were adjusted so that the delivered 5-FU amount was 2.5 mg per animal.

MRI Follow-up

Experiments were performed with a Bruker Avance DRX 300 (Bruker, Wissembourg, France) equipped with a vertical superwide-bore magnet operating at 7 T. T_2-weighted MR images of the brain were obtained using a multi-spin echo sequence with an in-plan resolution of 234 μm (TR = 2500 ms; TE = 15, 30, 45, 60, 75, 90, 105, and 120 ms, 9 to 11 contiguous slices of 1 mm, 2 acquisitions) (16). MR imaging was performed under isofluroane/oxygen anesthesia (2–5%/3l min^{-1}) on Day 10 to ensure tumor presence prior to treatment. Then, tumor progression was evaluated once a week.

Radiotherapy

On Day 12, animals were randomly divided into 4 groups: controls (untreated, n = 12), radiotherapy alone (RDT, n = 12), fast-release microspheres + radiotherapy (RDT + MS-F, n = 12) and slow-release microspheres + radiotherapy (RDT + MS-S, n = 7). Fractionated radiotherapy, carried out with a linear accelerator (Saturne 41, Varian Medical Systems, Salt Lake City, USA), consisted of 36 Gy given in 9 fractions over 3 weeks, and was initiated on Day 13. To limit radiotherapy toxicity, only hemibrain irradiations were performed under deep sedation of the animals (xylazine/ketamine), the rats being placed in a homemade device to ensure reproducibility of positioning and therefore irradiating areas.

Histology

Brains were rapidly gathered following animal sacrifice and kept at +4°C in formaldehyde 5% before further processing. Four-micrometer-thick coronal sections were prepared and stained by hematoxylin-eosin. The nature and extent of brain tumors, as well as the eventual presence of necrosis, hemorrhage and hemosiderosis and their respective gradings were evaluated (from 1: very few/slight to 5: severe).

Data Analysis and Statistics

The Bruker Paravision 2.1 software (Bruker, Wissembourg, France) was used to calculate tumor volumes by manual contour analysis on the T_2-weighted images and was also used to calculate quantitative transverse relaxation times (16). Statistical analysis was performed using a bi-factorial analysis of variance (ANOVA) with a multiple least-square analysis if required. The Student's *t*-test was used for comparing mean values.

RESULTS

Survival Data

Figure 1 presents survival data according to the Kaplan-Meier analysis. Rats surviving more than 120 days without evidence of pathologic development were sacrificed for brain histology examination and complete autopsy, and are henceforward named "long surviving." The median survival, as well as the survival extent, of animals receiving radiotherapy alone was significantly ($p < 0.05$) higher than for untreated animals (Table I). The presence of unloaded microspheres during tumor irradiation did not change any of the results (n = 3, data not shown). For 5-FU microsphere treated rats, survival medians and means were significantly different from the control group values ($p = 0.005$, Table I) but were not statistically different one from the other ($p = 0.43$). Nevertheless, a tendency existed showing that, when associated with radiotherapy, the slower the 5-FU release, the longer the survival. Long surviving animals were 0/12 in the control group and 1/12 in the radiotherapy group, as compared to 9/19 for 5-FU–loaded microsphere treated rats, given 5/12 (41%) in the MS-F treated group and 4/7 (57%) in the MS-S treated group (Fig. 1). For purposes of comparison, survival at 120 days was 27% and 0%, respectively, in the MS-F and MS-S treated groups without radiotherapy (15), which happened to be the contrary tendency than what was observed in the present study.

Histologic reports showed that 100% rats sacrificed due to the decline of their clinical status exhibited a malignant glioma or neoplastic reminiscence (Table II). Necrosis, grades 3–5, and hemorrhage, grades 1–2, were also noted. For rats surviving more than 120 days, neither tumor development nor reminiscence was described. 2/5 in the MS-F treated group exhibited necrosis grade 4 and hemosiderosis grade 1. One of four in the MS-S treated group showed necrosis grade 4. The remaining animals did not display any brain lesions.

Five of 12 radiotherapy-treated, 5/12 MS-F treated and

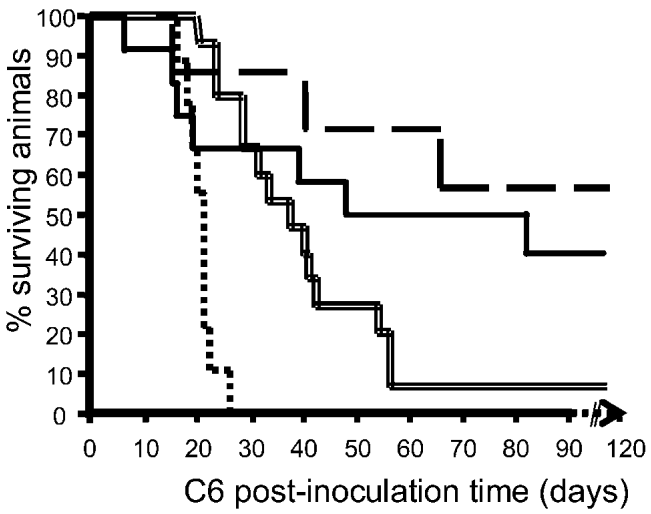

Fig. 1. Survival data presented according to the Kaplan-Meier analysis, as a function of time post-C6 cell inoculation, for control animals (n = 12, dotted line), group radiotherapy alone (n = 12, broken line), group radiotherapy + MS-F (n = 12, plain line), or group radiotherapy + MS-S (n = 7, dashed line).

Table I. Survival Data of C6-Bearing Rats Treated by Different Modalities

Group	n	Median (d)	Mean ± SD (days)	Survival interval (days)
Untreated	12	21	21 ± 3	[16–26]
RDT	11	36	38 ± 12	[21–57]
	1			>120
RDT + MS-F	7	28	41 ± 26	[15–91]
	5			>120
RDT + MS-S	3	49	49 ± 26	[24–75]
	4			>120

Survival data following the C6 inoculation of the various treated rats; RDT: fractionated radiotherapy alone; RDT + MS-F: radiotherapy + fast-release microspheres; RDT + MS-S: radiotherapy + slow-release microspheres; SD: standard deviation.

1/7 MS-S treated animals were not able to complete the radiotherapy cycle, due to rapid weight loss and marked prostration. They were subsequently sacrificed. Two of these sacrificed rats also manifested epileptic seizures during this period, 1/12 in the RDT group and 1/12 in the RDT + MS-F group.

Tumor Volume Development

All the animals tested positively for tumor presence 10 days after glioma cell injection, by MRI. 31 of them were subsequently followed for tumor development: 12/12 from the control group, 5/12 from the RDT group, 7/7 from the RDT + MS-S group and 7/12 from the RDT+ MS-F group, among which 3/7 were qualified as long surviving animals. On Day 10, tumors grew mainly along the needle track and their sizes were estimated at 13 ± 2 mm^3 ($n = 43$) on the multi-spin echo set of images. The tumors appeared as a homogeneous, hyper-intense spot in the left striatum of the rat brains (Figs. 2, 3, and 4) and were unambiguously characterized by an increase in the transverse relaxation time ($T_2^{tumor} = 56.4 \pm 0.8$ ms, mean ± SD; controlateral hemisphere, $T_2 = 54.3 \pm 0.3$ ms, mean ± SD, $p < 0.05$).

For radiotherapy-treated animals (long survivors excluded), the tumor volume curve displayed a biphasic exponential tendency (Fig. 5). From Day 10 to Day 29, the mean time for the tumor to double in size, calculated after Ross *et al.* (17), was 6 days. From Day 29, tumor development slowed, with a mean tumor doubling time of 24 days. T_2 values increased up to a mean value of 90 ± 22 ms at the last MR analysis (Day 43). The long-surviving rat displayed an increasing tumor volume from Day 10 to Day 36 (380 mm^3) and then a decreasing volume, finishing with only a small hyperintense pocket located at the previous tumor site at the last imaging point (Day 115).

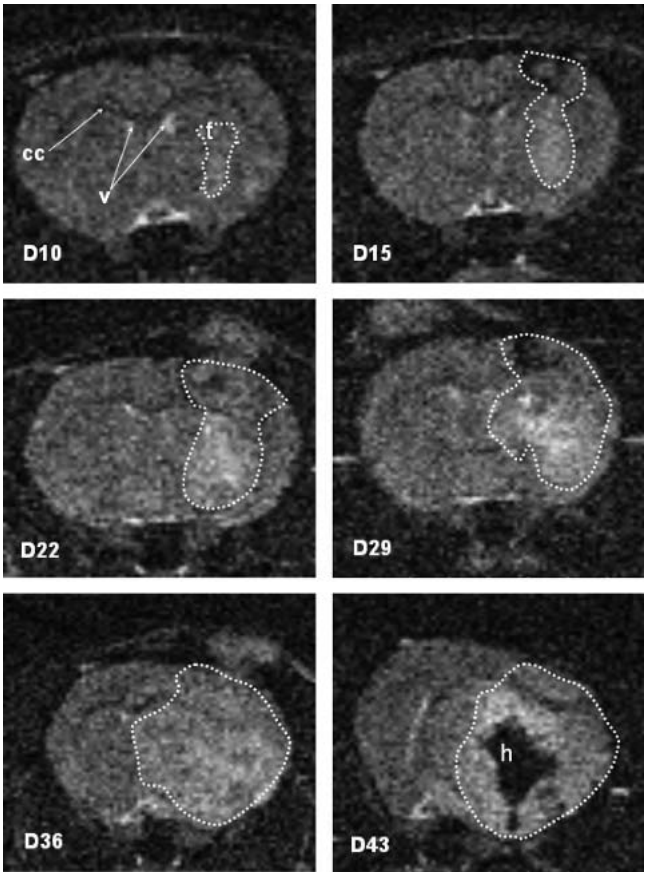

Fig. 2. Typical T_2-weighted MR images (TE = 60 ms) of the brain of a C6-glioma bearing rat prior to (D10), 2 (D15), 9 (D22), 16 (D29), 23 (D36), and 30 days (D43) after the beginning of the fractionated radiotherapy cycle (on D13). cc: corpus callosum; v: ventricle; t: tumor lesions; h: hemorrhage/hemosiderosis.

Figure 3 shows typical MR images of the brain of a C6-glioma bearing rat prior to, 2, 9, 16, 23 and 102 days after the beginning of radiotherapy (Day 13) in the presence of fast-

Table II. Histological Analyses of the Various Treated Groups

	n	Survival (days)	Malignant glioma	Neoplastic reminiscence	Necrosis	Hemorrhage	Hemosiderosis
RDT	9	[21–57]	Yes		3–5, n = 5	1, n = 1	NF
	2	[38–43]	NF	Yes	3–5, n = 2	2, n = 1	NF
	1	>120	NF	NF	NF	NF	NF
RDT + MS-F	7	[15–91]	Yes		4–5, n = 7	1–3, n = 7	1–3, n = 7
	5	>120	NF	NF	4, n = 2	NF	1, n = 2
RDT + MS-S	3	[24–75]	Yes		4, n = 1	NF	NF
	4	>120	NF	NF	NF	NF	1, n = 2

Brain histological data at necropsy. n: number of observations/subgroup; NF: not found.
Necrosis, hemorrhage, and hemosiderosis were scored from 1: very few/slight traces to 5: very severe/large areas.

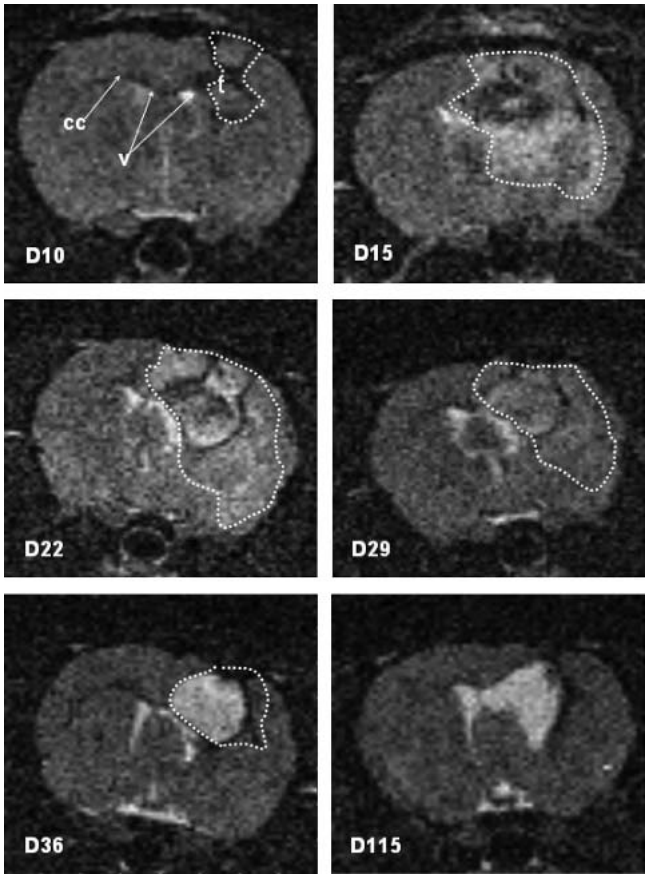

Fig. 3. Typical T_2-weighted MR images (TE = 60 ms) of the brain of a C6-glioma bearing rat, treated by MS-F microspheres on Day 12 (D12), prior to (D10), 2 (D15), 9 (D22), 16 (D29), 23 (D36), and 102 days (D115) after the beginning of the fractionated radiotherapy cycle (on D13). cc: corpus callosum; v: ventricle; t: tumor lesions.

release microspheres, whereas Fig. 4 shows typical MR images of the brain of a C6-glioma bearing rat prior to, 6, 13, 20, 41 and 102 days after the beginning of radiotherapy in the presence of slow-release microspheres. Both treatments gave similar patterns in terms of tumor volumes (Fig. 5): an exponential increase (mean doubling time: 3–6 days) followed by a plateau (200–300 mm^3) from Day 20 to Day 36, which corresponds to the end of the radiotherapy cycle. For animals surviving more than 40 days, the curves started to exhibit an exponential decrease, characterized by a slow mean half-dividing time of 24–27 days.

T_2 values followed the same pattern, being 56.4 ± 0.8 ms (n = 14) on Day 10, 76 ± 6ms (n = 11) on Day 36 decreasing to 58 ± 1 ms (n = 7) by Day 115 versus normal controlateral tissues, T_2^{normal} = 57.3 ± 0.9 ms (n = 7). Rats treated by the association radiotherapy–MS-F exhibited major hypersignals surrounding the tumor core from Day 15 to 36 (Fig. 3). At the final imaging point (Day 115, Fig. 3), an important hyperintense spot was visible at the tumor site for all the rats (n = 3), for which the T_2 estimated value (180 ms) was consistent with that estimated for ventricular liquid (200ms). On the contrary, MS-S treated brains showed almost no tumor lesion after Day 36 (Fig. 4). On Day 115, no pathologic lesion could be observed, except for a very slight healing scar along the needle track (n = 3, Fig. 4) or a similar hyperintense zone as for MS-F treated brains (n = 1).

DISCUSSION

Evaluating the synergistic action of two therapeutic agents *in vivo* may not be easy (18). Nevertheless, an agreement on results can be achieved if both treatments administered concomitantly produce a significant improvement in survival data compared to each single agent, without potentiating toxicities. In our case, we chose to examine three endpoints to determine the *in vivo* radiosensitization efficiency by 5-FU microspheres: complete remission rates; associated toxicity; and tumor volume evolution.

Toxicity manifestations (weight-loss, prostration) were noted in all groups, but were particularly exacerbated in the untreated and the radiotherapy only groups as well as in the presence of fast-release microspheres. These findings were not observed in a previous study evaluating 5-FU–loaded microsphere intrinsic efficacy on an established C6-glioma (15). In the present study, numerous necrotic brain areas were noticed at necropsy, an obviously aggravated phenomenon compared to previous studies. This bears witness to toxicity which could not be solely attributed to 5-FU microspheres or to the development of the C6 gliomas. Epileptic seizures occurred at similar levels in control and MS-F treated animals, which suggested that toxicity was more linked to radiotherapy than to 5-FU. One of the major drawbacks of radiotherapy remains

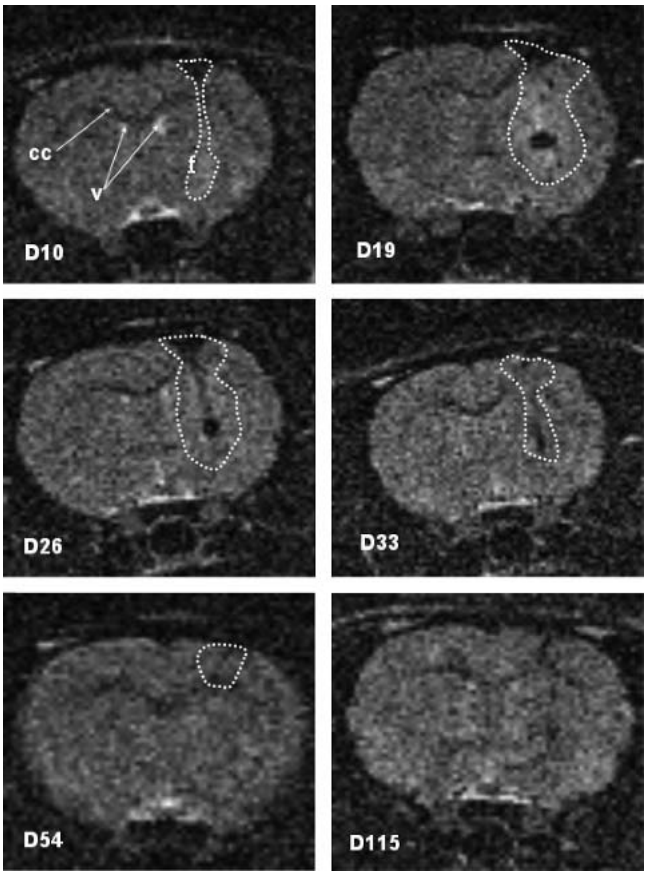

Fig. 4. Typical T_2-weighted MR images (TE = 60 ms) of the brain of a C6-glioma bearing rat, treated by MS-S microspheres on Day 12 (D12), prior to (D10), 6 (D19), 13 (D26), 20 (D33), 41 (D54), and 102 days (D115) after the beginning of the fractionated radiotherapy cycle (on D13). cc: corpus callosum; v: ventricle; t: tumor lesions.

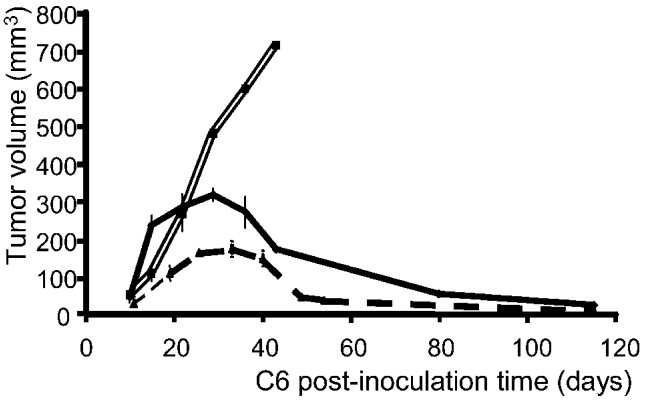

Fig. 5. Comparison of the mean evolution of tumor volume as a function of time following C6 cell inoculation for C6-glioma bearing rats: RDT-treated rats (n = 6, double line), RDT + MS-F treated animals (n = 7, plain line), and RDT + MS-S treated rats (n = 7, dashed line). Mean tumor volumes are given ± the standard error of the mean.

the consecutive cerebral edema in the absence of corticosteroid therapy and therefore, the over-estimation, by T_2-weighted MRI, of tumor volumes since tumor tissue contours and edema limits can not be separated precisely. However, adjuvant corticosteroid therapy was not chosen in order to allow a direct comparison of results with the previous studies (which permitted the assessment of intrinsic 5-FU microsphere efficiency) where no adjuvant therapy was administered. Moreover, although tumor volumes increased significantly in the few days following the beginning of radiotherapy, mean doubling times remained far lower than those observed in untreated animals or animals treated only with microspheres (14–16). This fact demonstrated the actual efficiency of radiotherapy only in slowing tumor growth.

MRI follow-up also enabled us to demonstrate the efficacy of associating radiotherapy and 5-FU microsphere use, by visualizing the decrease of tumor lesions as early as Day 26 (mid-radiotherapy cycle) for MS-S treated animals, and Day 36 (end of radiotherapy cycle) for MS-F treated rats. The different impact of the microsphere formulation on brain tissues was clearly illustrated. Fast-release microspheres, that is, producing a high 5-FU release in the first 24 h and a complete release within the first half of the radiotherapy cycle, seemed to generate a stronger edema (Fig. 2, Days 15 to 29) and a higher rate of brain necrosis (Table II). On the contrary, MS-S treated brains, that is, releasing 5-FU over a 3-week period with a lower drug release over the first 24 h, demonstrated less edema formation and a complete disappearance of lesions in 3/4 of those rats surviving more than 120 days, as confirmed by histology (Table II).

This tendency was in accordance with remission rates. Radiotherapy alone was able to cure 1/12 rats (8%), for which tumor presence had been confirmed at Day 10 (MRI analysis). The association with 5-FU–loaded microspheres dramatically increased the success of the therapeutic scheme: 41% and 57% for MS-F and MS-S treated animals, respectively. However, survival rates, toxic side effects, and tumor volumes tended to show that slow-release microspheres presented a greater and more interesting potential than fast-release systems. Even if these findings seemed to differ from previous results (14,15), they do not contradict them either, since it was previously found that a 5-FU bolus alone was not able to postpone C6 glioma growth for more than 4 days, providing evidence that the drug residence period in the tumor vicinity was not sufficient for a strong anti-tumor response. Thus, our present results indicate that, as part of an efficient therapeutic strategy, it seems important to favor the presence of the radiosensitizer 5-FU during the whole radiotherapy cycle with respect to a massive concentration of the anti-tumor agent at the beginning of radiotherapy.

The causes of this discrepancy are to be found in the intracerebral consequences of radiotherapy. Irradiation energy caused damage to tumors as well as to healthy cells. Repair mechanisms could restore cell gene information integrity but the presence of 5-FU induced new errors, increasing the chances to orientate the cell cycle toward death (9,19). This phenomenon was probably more beneficial in the case of MS-S treated brains because drug release covered a longer period than MS-F (3 weeks vs. 1 week *in vitro*).

Nevertheless, other parameters could also contribute to explain the better results observed with MS-S microspheres. For example, polymer degradation could have been speeded up by the energy provided by radiotherapy, in a similar way to that found for gamma-irradiation (20), although to a far lesser extent. Indeed, while the irradiation intensities concerned herein are about 100 times less important than the ones used for sterilization purposes, the presence of water and generated free radicals in the brain environment could partially reinforce the phenomenon. The resulting accelerated degradation would lead to shorter chain formation, facilitating the diffusion of small molecules, like water and 5-FU. Thus, fast-release microspheres, characterized by a porous morphology, with crystals concentrated near the microsphere surface, would release the drug in a markedly accelerated manner as compared to slow-release microspheres, whose external appearance was smoother, with 5-FU crystals more homogeneously entrapped in PLGA matrix (15). The massive release of 5-FU would be detrimental to the sustained release profile, resulting in faster disappearance of the drug in the tumor vicinity. However, the longer the 5-FU was released, the more beneficial it was, i.e., in the case of slow-release microspheres. Similarly, edema formation, while causing clinical deterioration of animals, may also have influenced local response to treatment since the increased extracellular water fraction may have reinforced convection movements and favored drug diffusion (21). However, once again, detrimental effects of edema seemed more significant when radiotherapy was associated with 5-FU fast-releasing microspheres as compared to a more moderate 5-FU release kinetics (MS-S).

All these events participated in explaining the superiority of the therapeutic association of radiotherapy/slow-release microspheres. The observed supra-additivity of actions between local 5-FU sustained delivery and fractionated radiotherapy remains very promising. After an encouraging pilot study (22), this strategy is presently under clinical investigation through a phase IIb multi-institutional randomized trial, for newly diagnosed glioblastoma patients who can undergo surgical resection. It also offers new hope for glioblastoma patients who suffer from deep, inoperable infiltrating tumors. This aspect of the strategy is similarly under clinical investigation.

ACKNOWLEDGMENTS

The authors would like to thank J. Haffner and N. Faisant for microsphere preparation, M. Berthy, P. Legras, and J. Roux for animal care assistance, and F. Franconi for MRI technical support, E. Germain for careful reading this manuscript. V.G.R. was supported by a grant by the Association pour la Recherche sur le Cancer (ARC, Villejuif, France).

REFERENCES

1. P. A. Forsyth and J. G. Cairncross. Treatment of malignant glioma in adults. *Curr. Opin. Neurol.* **8**(6):414–418 (1995).
2. P. L. Kornblith and M. Walker. Chemotherapy for malignant gliomas. *J. Neurosurg.* **68**(1):1–17 (1988).
3. S. Leibel and C. Scott. J. Loeffer. Contemporary approaches to the treatment of malignant gliomas with radiation therapy. *Semin. Oncol.* **21**:198–219 (1994).
4. B. Kimler. The 9L rat brain tumor model for pre-clinical investigations of radiation-chemotherapy interactions. *J. Neurooncol.* **20**:103–109 (1994).
5. E. Douple. Platinum-radiation interactions. *Nat. Cancer Inst. Mono.* **6**:315–319 (1988).
6. C. Coughlin, C. Scott, C. Langer, L. Coia, W. Curran, and P. Rubin. Phase II, two-arm RTOG trial (94-11) of bischloroethyl-nitrosourea plus accelerated hyperfractionated radiotherapy (64.0 or 70.4 Gy) based on tumor volume in the treatment of newly-diagnosed radiosurgery-ineligible glioblastoma multiforme patients. *Int. J. Radiat. Oncol. Biol. Phys.* **48**(5):1351–1358 (2000).
7. S. Madajewicz, N. Chowhan, A. Tfayli, C. Roque, A. Meek, R. Davis, W. Wolf, C. Cabahug, P. Roche, J. Manzione, A. Iliya, M. Shady, P. Hentschel, H. Atkins, and A. Braun. Therapy for patients with high grade astrocytoma using intraarterial chemotherapy and radiation therapy. *Cancer* **88**(10):2350–2356 (2000).
8. V. A. Levin, M. R. Prados, W. M. Wara, R. L. Davis, P. H. Gutin, T. L. Phillips, K. Lamborn, and C. B. Wilson. Radiation therapy and bromodeoxyuridine chemotherapy followed by procarbazine, lomustine and vincristine for the treatment of anaplasic gliomas. *Int. J. Rad. Oncol. Biol. Phys.* **32**(1):75–83 (1995).
9. L. Hughes, J. Luengas, T. Rich, and D. Murray. Radiosensitization of cultured human colon adenocarcinoma cells by 5-fluorouracil: effects on cell survival, DNA repair and cell recovery. *Int. J. Radiat. Oncol. Biol. Phys.* **23**(5):983–991 (1992).
10. R. Schilsky. Biochemical pharmacology of chemotherapeutic drugs used as radiation enhancers. *Semin. Oncol.* **19**(4 suppl 11): 2–7 (1992).
11. P. McSheehy and J. Griffiths. 19F MRS studies of fluoropyrimidine chemotherapy. A review. *NMR Biomed.* **2**:133–141 (1989).
12. M. Boisdron-Celle, P. Menei, and J. P. Benoit. Preparation and characterization of 5-fluorouracil-loaded microparticles as biodegradable anticancer drug carriers. *J. Pharm. Pharmacol.* **47**:108–114 (1995).
13. P. Menei, M. Boisdron-Celle, A. Croué, G. Guy, and J. P. Benoit. Effect of stereotactic implantation of biodegradable 5-fluorouracil-loaded microspheres in healthy and C6 glioma-bearing rats. *Neurosurgery* **39**(1):117–123 (1996).
14. L. Lemaire, V. G. Roullin, F. Franconi, M. C. Venier-Julienne, P. Menei, P. Jallet, J. J. Le Jeune, and J. P. Benoit. Therapeutic efficiency of 5-fluorouracil-loaded microspheres on rat glioma: a magnetic Resonance Imaging study. *NMR Biomed.* **14**(6):360–366 (2001).
15. V. G. Roullin, L. Lemaire, M. C. Venier-Julienne, N. Faisant, F. Franconi, and J. P. Benoit. Release kinetics of 5-fluorouracil-loaded microspheres on an experimental rat glioma. *Anticancer Res.* **23**(1A):21–25 (2003).
16. L. Lemaire, F. Franconi, J. P. Saint-André, V. G. Roullin, P. Jallet, and J. J. Le Jeune. High-field quantitative transverse relaxation time, magnetization transfer and apparent water diffusion in experimental rat brain tumour. *NMR Biomed.* **13**(3): 116–123 (2000).
17. B. D. Ross, Y. J. Zhao, E. R. Neal, L. D. Stegman, M. Ercolani, O. Ben-Yoseph, and T. L. Chenevert. Contribution of cell kill and posttreatment tumor growth rates to the repopulation of intracerebral 9L tumors after chemeotherapy: an MRI study. *Proc. Natl. Acad. Sci. USA* **95**:7012–7017 (1998).
18. T. C. Chou and D. C. Rideout. *Synergism and antagonism in chemotherapy*, Academic Press, San Diego, 1991.
19. L. Li, H. Nakajima, and T. Nomura. Dose rate effectiveness and potentially lethal damage repair in normal and double-strand break repair deficient murine cells by gamma-rays and 5-fluorouracil. *Cancer Let.* **123**:227–232 (1998).
20. N. Faisant, J. Siepmann, J. Richard, and J. P. Benoit. Mathematical modeling of drug release from bioerodible microparticles : effect of gamma-irradiation. *Eur. J. Pharm. Biopharm.* **56**:271–279 (2003).
21. L. K. Fung, M. Shin, B. Tyler, H. Brem, and W. M. Saltzman. Chemotherapeutic drugs released from polymers: distribution of 1,3-bis(2-chloroethyl)-1-nitrosourea in the rat brain. *Pharm. Res.* **13**(5):671–682 (1996).
22. P. Menei, M. C. Venier, E. Gamelin, J. P. Saint-Andre, G. Hayek, E. Jadaud, D. Fournier, P. Mercier, G. Guy, and J. P. Benoit. Local and sustained delivery of 5-fluorouracil from biodegradable microspheres for the radiosensitization of glioblastoma. *Cancer* **86**(2):325–330 (1999).